

Design Your Own Universe: A Physics-Informed Agnostic Method for Enhancing Graph Neural Networks

Dai Shi ^{*†} Andi Han ^{‡*} Lequan Lin ^{*‡} Yi Guo [§] Zhiyong Wang [†] Junbin Gao [†]

Abstract

Physics-informed Graph Neural Networks have achieved remarkable performance in learning through graph-structured data by mitigating common GNN challenges such as over-smoothing, over-squashing, and heterophily adaption. Despite these advancements, the development of a simple yet effective paradigm that appropriately integrates previous methods for handling all these challenges is still underway. In this paper, we draw an analogy between the propagation of GNNs and particle systems in physics, proposing a model-agnostic enhancement framework. This framework enriches the graph structure by introducing additional nodes and rewiring connections with both positive and negative weights, guided by node labeling information. We theoretically verify that GNNs enhanced through our approach can effectively circumvent the over-smoothing issue and exhibit robustness against over-squashing. Moreover, we conduct a spectral analysis on the rewired graph to demonstrate that the corresponding GNNs can fit both homophilic and heterophilic graphs. Empirical validations on benchmarks for homophilic, heterophilic graphs, and long-term graph datasets show that GNNs enhanced by our method significantly outperform their original counterparts.

1 Introduction

Graph Neural Networks (GNNs) have demonstrated exceptional performance in learning tasks involving graph-structured data [40, 20, 32, 27]. Recent studies in the GNN domain have unveiled a connection between continuous physical diffusion processes and their discretized versions on graphs [8, 21]. Accordingly, numerous physics-informed methods have been proposed to mitigate issues in GNN such as over-smoothing (OSM) [41], over-squashing (OSQ) [42], and heterophily adaptation [11]. Specifically, in addressing the OSM problem, one needs to ensure that node features remain distinguishable after several iterations of GNN [6, 31]. To achieve this, it may be necessary for some connected nodes to “repulse” each other, so they can be categorized into different classes from GNN outputs [45, 16]. Methods that enable GNNs to do this naturally enhance the networks’ ability to adapt to heterophily graphs, in which connected nodes are more likely to belong to different classes of labels. On the other hand, to mitigate OSQ issues, it is crucial to allow information to flow more effectively through GNN propagation [37]. This can be accomplished by leveraging strategies such as graph adjacency rewiring and reweighting based on topological features like curvatures [42, 14, 35] and spectral expanders [26, 5, 3]. Additionally, it has been observed that there is a

^{*}Equal contributions for the first three authors.

[†]University of Sydney, (dai.shi, lequan.lin, zhiyong.wang, junbin.gao@sydney.edu.au)

[‡]andi.han@riken.jp

[§]Western Sydney University, (y.guo@westernsydney.edu.au).

trade-off between the OSM and OSQ issues in GNNs, leading to a few recent studies to focus on alleviating both issues simultaneously [33, 19].

Based on the aforementioned contents, to mitigate both OSM and OSQ problems, one may prefer to leverage a mixed operation that involves graph rewiring to reduce the OSQ issue and induce repulsive forces between nodes to alleviate OSM issues. In this paper, inspired by the field of particle systems in physics, we introduce a novel model agnostic paradigm that leverages node labeling information to induce both repulsive forces and rewiring on the graph. Our approach can be applied to many GNNs for deep learning on graphs.

Contributions First, we introduce the notion of collapsing nodes (CNs) that served as reliable “gravitational” sources via GNNs training. We show that guided by the node labeling information, the graph adjacency, expanded by the CNs, makes the propagation of GNNs through both attractive and repulsive forces. Second, we theoretically verify that our proposed models can mitigate both OSM and OSQ issues and the heterophily adaption problem. We also discuss the spectral property of the CNs rewired graph and show that it is those negative eigenvalues that enhance our models’ adaption power to heterophilic graphs. Furthermore, we show the impact of CNs via graph curvature and the trade-off relation between OSM and OSQ problems. Lastly, we conduct various experiments to demonstrate the effectiveness of our method on both homophilic and heterophilic graphs as well as long-term learning tasks.

2 Preliminary

Graph Basics and Graph Homophily Let $\mathcal{G} = (\mathcal{V}, \mathcal{E}_0)$ represent an connected undirected graph with N nodes, where \mathcal{V} and \mathcal{E}_0 denote the sets of nodes and edges, respectively. The adjacency matrix $\mathbf{A} \in \mathbb{R}^{N \times N}$ is defined such that $a_{i,j} = 1$ if $(i, j) \in \mathcal{E}_0$ and zero otherwise. We introduce $\mathbf{X} \in \mathbb{R}^{N \times d_0}$ to represent the matrix of d_0 -dimensional nodes features, with $\mathbf{x}_i \in \mathbb{R}^{d_0}$ as its i -th row (transposed). Additionally, we define $\mathbf{Y} \in \mathbb{R}^{N \times C}$ as the node label matrix, comprising label vectors for the labeled nodes (via one-hot coding) and zero vectors for the unlabeled nodes, where C is the total number of classes. Apart from these basic notations on graph, we also recall the notion of so-called graph homo/heterophily, which shows how labels are distributed among connected nodes.

Definition 1 (Homophily and Heterophily). The homophily or heterophily of a network is used to define the relationship between labels of connected nodes. Denote $\mathcal{N}_i \subseteq \mathcal{V}$ as the neighbors of node i . The level of homophily of a graph is measured by the positive score $\mathcal{H}(\mathcal{G}) = \mathbb{E}_{v_i \in \mathcal{V}}[|\{v_j : v_j \in \mathcal{N}_i \text{ and } y_j = y_i\}|/|\mathcal{N}_i|]$. A score $\mathcal{H}(\mathcal{G})$ close to 1 corresponds to strong homophily while a score $\mathcal{H}(\mathcal{G})$ nearly 0 indicates strong heterophily. We say that a graph is a homophilic (heterophilic) graph if it has stronger homophily (heterophily), or simply strong homophily (heterophily).

Based on the definition of graph homophily, one can see that, compared to homophily graphs which require a learning model to predict nearly identical labels to connected nodes, distinct label predictions are preferred for heterophilic graphs.

MPNNs and Graph Neural Diffusion Consider node i with feature representation $\mathbf{h}_i^{(\ell)}$ at layer ℓ , and $\mathbf{h}_i^{(0)} = \mathbf{x}_i$. Message Passing Neural Networks (MPNNs) [17] use message functions $\psi_\ell : \mathbb{R}^{d_\ell} \times \mathbb{R}^{d_\ell} \rightarrow \mathbb{R}^{d'_\ell}$

and update functions $\phi_\ell : \mathbb{R}^{d_\ell} \times \mathbb{R}^{d'_\ell} \rightarrow \mathbb{R}^{d_{\ell+1}}$ defined by:

$$\mathbf{h}_i^{(\ell+1)} = \phi_\ell \left(\mathbf{h}_i^{(\ell)}, \sum_{j \in \mathcal{N}_i} \mathbf{A}_{ij} \psi_\ell(\mathbf{h}_i^{(\ell)}, \mathbf{h}_j^{(\ell)}) \right). \quad (1)$$

It is worth noting that \mathbf{A} can be replaced with the features that are defined on the edges of the graph. For the simplicity of our analysis, we only consider MPNNs with \mathbf{A} included. Classical GNNs like GCN [27] and GAT [43] are the examples of this MPNN framework. Crucially, MPNNs also act as solvers for discrete dynamics on graphs, like the well-known graph neural diffusion [8, 41]. Specifically, [8] incorporated the message passing scheme and its variants in their GRAND models as described as:

$$\frac{\partial}{\partial t} \mathbf{h}(t) = \text{div}(\mathbf{G}(\mathbf{h}(t), t) \nabla \mathbf{h}(t)), \quad (2)$$

where $\mathbf{G}(\mathbf{h}(t), t) = \text{diag}(a(\mathbf{h}_i(t), \mathbf{h}_j(t), t))$ in which a denotes a function that quantifies the similarity between node features, such as the attention coefficient [43]. We further let $\nabla \mathbf{h}$ represents the graph gradient operator, defined as $\nabla : L^2(\mathcal{V}) \rightarrow L^2(\mathcal{E}_0)$ such that $(\nabla \mathbf{h})_{ij} = \mathbf{h}_j - \mathbf{h}_i$, where $L^2(\mathcal{V})$ and $L^2(\mathcal{E}_0)$ be Hilbert spaces for real-valued functions on \mathcal{V} and \mathcal{E}_0 , respectively with the inner products given by

$$\langle f, g \rangle_{L^2(\mathcal{V})} = \sum_{i \in \mathcal{V}} f_i g_i, \quad \langle F, G \rangle_{L^2(\mathcal{E}_0)} = \sum_{(i,j) \in \mathcal{E}_0} F_{ij} G_{ij},$$

for $f, g : \mathcal{V} \rightarrow \mathbb{R}$ and $F, G : \mathcal{E}_0 \rightarrow \mathbb{R}$. Similarly, we denote graph divergence $\text{div} : L^2(\mathcal{E}_0) \rightarrow L^2(\mathcal{V})$, being the inverse of graph gradient operator, is defined as $(\text{div} F)_i = \sum_{j:(i,j) \in \mathcal{E}_0} F_{ij}$.

3 Motivations and Model Formulation

3.1 Graph Diffusion as Particle System

Let us go deeper to the scheme of GRAND presented in (2), one can rewrite (2) into a component-wise form such that

$$\frac{\partial}{\partial t} \mathbf{h}_i = \sum_{j \in \mathcal{N}_i} a(\mathbf{h}_i, \mathbf{h}_j) (\mathbf{h}_j - \mathbf{h}_i), \quad (3)$$

where we drop time t from now on for the ease of notation. It suggests that the dynamic of the change of the feature of node i is conducted by aggregating its neighbouring information, suggesting a homogenizing process on the connected nodes. Furthermore, similar to the work in [45], one can interpret (3) as an interactive particle system, in which all particles (nodes) attracted each other and eventually, after sufficient propagation, collapsed into one overlapped node with fixed feature, as long as we have the similarity score (i.e., $a(\mathbf{h}_i, \mathbf{h}_j)$) positive throughout the propagating process. Although such feature processing might be friendly to homophily graphs, it is not hard to see that it may not be necessary for heterophily graphs, in which adjacent nodes are preferred to be pushed apart from each other, resulting in more distinctive node features. Accordingly, the recent work [45] enhances (3) by including negative similarities (i.e., negative edge weights) such that

$$\frac{\partial}{\partial t} \mathbf{h}_i = \sum_{j \in \mathcal{N}_i} (a(\mathbf{h}_i, \mathbf{h}_j) - \beta_{i,j}) (\mathbf{h}_j - \mathbf{h}_i) + \delta \mathbf{h}_i (1 - \mathbf{h}_i^2), \quad (4)$$

in which $\beta_{i,j}$ is leveraged to adjust the sign of $(a(\mathbf{h}_i, \mathbf{h}_j) - \beta_{i,j})$ so that the particle system can adopt both attractive and repulsive forces. The additional term $\mathbf{h}_i(1 - \mathbf{h}_i^2)$ is the double-well potential that is widely used in quantum particle physics [24] to prevent the so-called energy explosion, serving as a physical barrier (bound) of the node feature variation. Although remarkable improvement in learning accuracy has been observed from the model defined in (4), it is still unknown that **what type of force is needed for a given node pair**. In fact, in [45], $\beta_{i,j}$ was simplified as a single constant hyper-parameter throughout the training. This opens a rich venue for future research to explore the criteria for determining the suitable type of force, which is measured by the sign of similarity for the given pair of nodes.

3.2 The Ideal Universe

To identify the criteria of determining the type of forces for a given node pair, ideally one shall prefer the particle system to be evolved as

All nodes with the same labels shall eventually collapse to one node with identical features. Nodes with different labels shall be apart from each other with distinctive features.

This requirement directly suggests leveraging the node labeling information as a guide to determine the type of force for one specific node pair during the training process. Below we introduce the notion of (label) collapsing nodes.

Definition 2 (Collapsing Nodes). Let $\mathcal{V} = \{v_1, \dots, v_N\}$ be the nodes in the input graph and \tilde{v} be a node with known label information \tilde{y} . \tilde{v} is a collapsing node (CN) if for any $v_i \in \mathcal{V}$ with known labels y_i , \tilde{v} is connected to v_i with positive weights if $\tilde{y} = y_i$ and negative weights if $\tilde{y} \neq y_i$ regardless of original connectivity.

The definition of collapsing nodes (CNs) suggests that by leveraging the known node label information, CNs serve as a “gravitational” source via the feature propagation, since all nodes with available label information are connected to CNs, and will be attracted/repulsed by CNs if they have the same/different labels. We further note that CNs can be either sourced from the node from the original graph or added as additional nodes to the graph. For the convenience of this study, in the sequel, we only consider the second type of CNs (additional nodes to the graph).

Accordingly, this augments the original graph by adding a connection matrix $\mathbf{C} \in \mathbb{R}^{N \times K}$ (for K collapsing nodes),

$$C_{i,k} = \begin{cases} +1, & \text{if } y_i \text{ known and } y_i = \tilde{y}_k \\ -1, & \text{if } y_i \text{ known and } y_i \neq \tilde{y}_k \\ 0, & \text{otherwise} \end{cases}$$

where we use \tilde{y}_k to denote the label of CN k for $k = 1, \dots, K$.

For convenience, we set K equal to C , the number of unique labels in a given graph. The corresponding adjacency matrix after including CNs is thus given by

$$\mathbf{A}_c = \begin{bmatrix} \mathbf{A} & \mathbf{C} \\ \mathbf{C}^\top & \mathbf{0} \end{bmatrix}. \quad (5)$$

Further if the adjacency includes self-loops, then $\mathbf{A}_c = \begin{bmatrix} \mathbf{A} & \mathbf{C} \\ \mathbf{C}^\top & \mathbf{1}_{K \times K} \end{bmatrix}$, where $\mathbf{1}_{K \times K}$ is a diagonal matrix (block) of size $K \times K$ with entries of all ones. Considering that \mathbf{A}_c contributes valuable node labeling

information to the propagation of node features, a **model-agnostic framework** can be established. We name such framework as **UYGNNs**, short for **Universal Label based (Y) Graph Neural Networks**. Accordingly, one can define **UYGCN** that propagates nodes features with the following dynamic

$$\frac{\partial}{\partial t} \mathbf{h}_i = \sum_{j \in \mathcal{N}_i} (a_c^{\text{GCN}}(\mathbf{h}_i, \mathbf{h}_j))(\mathbf{h}_j - \mathbf{h}_i), \quad (6)$$

where $a_c^{\text{GCN}}(\mathbf{h}_i, \mathbf{h}_j)$ denotes the edge similarities contained in \mathbf{A}_c . Note that here the index i runs through all the $N + K$ nodes and \mathcal{N}_i includes the neighbours of node i from the extended edge set $\hat{\mathcal{E}} = \mathcal{E}_0 \cup \mathcal{E}_1$, where \mathcal{E}_1 denotes the set of edges of connecting nodes with label information available to CNs. Similarly, attention mechanism [43] can be deployed into the above message passing scheme. In this case, one can further define the dynamic of **UYGAT** as

$$\frac{\partial}{\partial t} \mathbf{h}_i = \sum_{j \in \mathcal{N}_i} (a_c^{\text{GCN}}(\mathbf{h}_i, \mathbf{h}_j) \cdot a_c^{\text{GAT}}(\mathbf{h}_i, \mathbf{h}_j)) \cdot (\mathbf{h}_j - \mathbf{h}_i), \quad (7)$$

where $a_c^{\text{GAT}}(\mathbf{h}_i, \mathbf{h}_j) > 0$ is the attention coefficient for the connected nodes pair (i, j) . The multiplication between a_c^{GCN} and a_c^{GAT} is leveraged to preserve the sign of the edge weights so that the type of forces can be maintained. Furthermore, to prevent the potential energy explosion in UYGNN models, similar to ACMP [45], double-well potential as well as other type of physical potential terms (e.g., harmonic oscillator potential [30]) can be leveraged to further restrict the motion of nodes.

3.3 An even More Complexed Universe

Apart from the structure of UYGCN and UYGAT, which only assigns repulsive force between NC and the nodes with different labels, node labeling information can also serve as a guide to assign repulsive forces on original graph connectivities. Specifically, one can achieve this by leveraging the label-based adjacency matrix \mathbf{A}_y , with its entries defined as

$$(\mathbf{A}_y)_{i,j} = \begin{cases} +1, & \text{if } y_i = y_j \\ -1, & \text{if } y_i \neq y_j \\ 0, & \text{otherwise} \end{cases}$$

for any edge pair $(i, j) \in \mathcal{E}$. The corresponding dynamic is

$$\frac{\partial}{\partial t} \mathbf{h}_i = \sum_{j \in \mathcal{N}_i^0} (a_y(\mathbf{h}_i, \mathbf{h}_j) \cdot a(\mathbf{h}_i, \mathbf{h}_j)) \cdot (\mathbf{h}_j - \mathbf{h}_i) + \sum_{j \in \mathcal{N}_i^1} a_c(\mathbf{h}_i, \mathbf{h}_j) \cdot (\mathbf{h}_j - \mathbf{h}_i), \quad (8)$$

where we denote \mathcal{N}_i^0 and \mathcal{N}_i^1 as the neighbors of node i from \mathcal{E}_0 and \mathcal{E}_1 , respectively. It is not hard to see that for any nodes with label information above, such universe design will ensure that nodes will **only** be attracted by those nodes with the same label and pushed away from nodes with different labels.

3.4 MLP in&out Paradigm

To implement the propagation according to the dynamic UYGNNs (i.e., (6)), one can conduct an MLP in-and-out paradigm [8] as follows.

$$\mathbf{H}^{(\ell)} = \text{MLP}_{\text{in}}^{(\ell)}(\mathbf{H}^{(\ell)}), \quad (9)$$

$$\mathbf{H}' = \sigma_{\ell}(\mathbf{A}_c \mathbf{H}^{(\ell)}), \quad (10)$$

$$\mathbf{H}^{(\ell+1)} = \text{MLP}_{\text{out}}^{(\ell)}(\mathbf{H}'), \quad (11)$$

where we have $\mathbf{H}^{(0)} = \mathbf{X}$. Practically, MLP_{in} and MLP_{out} are implemented with two learnable channel mixing matrices $\mathbf{W}_{\text{in}}^{(\ell)} \in \mathbb{R}^{d_{\ell} \times d'_{\ell}}$ and $\mathbf{W}_{\text{out}}^{(\ell)} \in \mathbb{R}^{d'_{\ell} \times d_{\ell+1}}$, respectively, and σ is the activation function. One can further check that the computational complexity of UYGNN is with $\mathcal{O}(|\hat{\mathcal{E}}|d'_{\ell})$, which is similar to the classic GNNs [27].

4 Theoretical Analysis of Y-GNNs

In this section, we theoretically verify that UYGNN can handle the aforementioned GNN issues, such as OSM, OSQ, and heterophily adaption. All proving details are included in Appendix A.

4.1 Avoiding OSM

We start our analysis by showing that UYGNN can avoid the OSM problem. Specifically, the dynamics of (6) can be shown to avoid OSM in the limit, i.e., not converging to a constant state. This can be read directly from the result that the constant state is not a stationary point of the dynamics. To see this, we consider normalized adjacency $\hat{\mathbf{A}}_c = \mathbf{D}_c^{-1}(\mathbf{A}_c + \mathbf{I})$ (for the symmetrically normalized adjacency, the idea is the same), where $(\mathbf{D}_c)_{ii} = \sum_j |(a_c)_{i,j}|$. Without loss of generality, consider a single feature $\mathbf{h} = [\mathbf{x}; \mathbf{f}]$ where $\mathbf{x} \in \mathbb{R}^N, \mathbf{f} \in \mathbb{R}^K$ represents the features of original nodes and added collapsing nodes. Thus (6) can be viewed as a system of (\mathbf{x}, \mathbf{f}) . In order for OSM to occur, there must exist a constant vector $\mathbf{c} = c\mathbf{1}_N$ such that $\mathbf{x} = \mathbf{c}$ as $t \rightarrow \infty$.

The next proposition shows that the constant state is not a limiting state of the dynamics we consider as long as there exists at least one training sample per class. This suggests OSM can be avoided.

Proposition 1. *Suppose K is equal to the number of classes and there exists at least one training sample per class. Consider the Euler discretized dynamics of (6) as the fixed point iteration $\mathbf{h}^{(\ell+1)} = \mathbf{A}_c \mathbf{h}^{(\ell)}$ where $\mathbf{h} \in \mathbb{R}^{N+K}$. Then the limit $\mathbf{h} = (\mathbf{c}, \bar{\mathbf{f}})$ of the iteration, the stationary point, is not in the form of $\mathbf{c} = c\mathbf{1}_N \in \mathbb{R}^N$ and $\bar{\mathbf{f}} \in \mathbb{R}^K$.*

One can verify that on one specific time t , the dynamic in (6) is the minimizer of the following energy

$$\begin{aligned} E^-(\mathbf{H}) &= \text{tr}(\mathbf{H}^{\top}(\mathbf{I} - \mathbf{A}_c)\mathbf{H}) = \sum_{i,j} (\mathbf{A}_c)_{i,j} \|\mathbf{h}_i - \mathbf{h}_j\|^2 \\ &= \sum_{(i,j) \in \mathcal{E}_0} \|\mathbf{h}_i - \mathbf{h}_j\|^2 + \sum_{(i,k) \in \mathcal{E}_1, y_i = y_k} \|\mathbf{h}_i - \mathbf{h}_k\|^2 - \sum_{(i,k) \in \mathcal{E}_1, y_i \neq y_k} \|\mathbf{h}_i - \mathbf{h}_k\|^2. \end{aligned}$$

This provides an intuitive explanation for the behaviour of our proposed dynamics, i.e., pushing samples from the same class to its corresponding collapsing node, while maximizing their separation from other collapsing

nodes. We further highlight that if we combine the energy $E^-(\mathbf{H})$ with the double-well potential term, then the energy becomes the popular Ginzburg-Landau energy [29]. However, $E^-(\mathbf{H})$ can be negative depending on the graph spectra, we provide a more detailed discussion on this phenomenon regarding GNN heterophily adaption in Section 4.3.

Cluster Flocking At the beginning of Section 3.2, we proposed the ideal evolution of the node features according to their labeling information, and we have verified that, based on our design, nodes propagated under UYGNNs move toward the consequences that we prefer to observe. Yet it is still unknown whether node features’ asymptotic states align with the criteria we proposed before. In Appendix B, we demonstrate that the UYGAT in (7) with double-well potential can asymptotically achieve the so-called *cluster flocking* [13] in which nodes with same labels will be clustered due to the attractive forces whereas nodes with different labels will be parted away because of the repulsive forces. However, it is unlikely for UYGNN to achieve cluster flocking. Similarly, determining the graph structure that guarantees node clustering flocking is a complex but exciting field to explore, and we leave it to future works.

Deal with energy explosion Similar to ACMP [45], the double-well potential helps to regulate the magnitude of Dirichlet energy, as shown in the following proposition.

Proposition 2. Denote $\mathcal{E}_{\text{dir}}(\mathbf{h}) = \mathbf{h}^\top \hat{\mathbf{L}} \mathbf{h}$ the Dirichlet energy of the signal on graph \mathcal{G} . Then there exist a constant depending only on N and the largest eigenvalue λ_{\max} of \mathbf{L} , such that $\|\mathbf{h}\|_2^2 \leq C$ and $\mathcal{E}_{\text{dir}}(\mathbf{h}) \leq \lambda_{\max} \|\mathbf{h}\|_2^2 \leq 2\|\mathbf{h}\|_2^2$, for some constant that depends on the node size.

4.2 Deal with OSQ

As CNs bring additional connectivities to the original graph, it is natural to explore the impact of these newly added edges on the so-called OSQ problem of GNNs. The OSQ issue of GNNs can be viewed as a type of information compression problem such that a large amount of feature information is compressed into a narrow path due to the graph topology, causing GNNs to fail to capture the long-term relationship between nodes [42, 5]. In this section, we measure the OSQ problem via the sensitivity score leveraged in [42, 5, 37], and show that with the help of CNs, UYGNNs could increase the OSQ score upper bound thus mitigate the OSQ problem. We further highlight that despite CNs bringing both attractive and repulsive forces by assigning different signs on edges, from the information transaction point of view, both types of these additional edges make the information “easier” to communicate. Accordingly, it is natural to measure the OSQ problem via $|\mathbf{A}_c|$ in which additional edges with negative weights are replaced by their absolute values. It is worth noting that, for the sake of convenience in analysis, we only consider one channel mixing matrix (i.e., \mathbf{W}_{in}), and our conclusion can be easily extended to the case for both \mathbf{W}_{in} and \mathbf{W}_{out} .

Proposition 3. Consider the UYGNN paradigm defined in (9) and (10). Assuming \mathcal{G} is not a bipartite graph, let $i, s \in \mathcal{V}$, if $|\sigma'_\ell| \leq \alpha$, $\|\mathbf{W}_{\text{in}}^{(\ell)}\| \leq \beta_{\text{in}}$ for $0 \leq \ell \leq r$, then

$$\left\| \frac{\partial \mathbf{h}_i^{(r)}}{\partial \mathbf{x}_s} \right\| \leq (2\alpha\beta_{\text{in}})^r \left(\sum_{\ell=0}^r |\mathbf{A}_c|^\ell \right)_{i,s}. \quad (12)$$

We highlight that our result can serve as an extension of Lemma 3.2 in [5] by considering the impact of negatively weighted edges in \mathbf{A}_c . We leave detailed proof and additional remarks in Appendix 3. Based on the conclusion in Proposition 3, one can see the additional edges induced from CNs densified the original graph adjacency \mathbf{A} , thus naturally resulting as a higher upper bound as expressed in (12).

4.3 Role of Laplacian Negative Eigenvalues

In this section, we delve deeper into the impact of the negative weighted edges on the graph spectra. Specifically, one can define the graph Laplacian $\mathbf{L}_c = \mathbf{E}\mathbf{W}_c\mathbf{E}^\top$ [10], where $\mathbf{E} \in \mathbb{R}^{(N+K) \times |\hat{\mathcal{E}}|}$ is the incidence matrix and $\mathbf{W}_c \in \mathbb{R}^{|\hat{\mathcal{E}}| \times |\hat{\mathcal{E}}|}$ is a diagonal matrix with entries of edge weights. Based on the form of the dynamics of UYGCN in (6), without considering the double-well potential term, one can explicitly write out the solution of the differential equation as¹

$$\mathbf{H}(t) = e^{-t\mathbf{L}_c}\mathbf{H}(0) = \mathbf{U}e^{-\mathbf{\Lambda}_c t}\mathbf{U}^\top\mathbf{H}(0), \quad (13)$$

where $\mathbf{\Lambda}_c$ is the diagonal matrix with entries of eigenvalues of the Laplacian. By assuming a discrete integer time t and replacing it with the number of layer ℓ , one can have the solution of the UYGCN, which serves as the discretized version of the dynamics in (6). Now, as we have included negative edge weights in \mathbf{A}_c , \mathbf{L}_c could have negative eigenvalues [10]. We highlight that this is exactly what UYGNN needs to fit heterophily graphs. Since from (13), one can treat $e^{-\mathbf{\Lambda}_c}$ as a spectral filter, and if the entries of $\mathbf{\Lambda}_c \geq 0$, then $e^{-\mathbf{\Lambda}_c}$ serves as a low-pass filtering function (monotonic decrease), which tends to homogenize the components of node features, whereas in the case when all $(\mathbf{\Lambda}_c)_{ii} < 0$ it becomes a high-pass filtering function (monotonic increase), which imposes sharpening effect on nodes features. Let \mathcal{G}_c be the graph with CNs additionally added, \mathcal{V}_c be the set of nodes of \mathcal{G}_c , and $\mathcal{T}(\mathcal{V}_c)$ be the training set. The following theorem provides insights into its Laplacian spectrum.

Theorem 1. *Assuming every additionally added CN has at most one node in the training set $\mathcal{T}(\mathcal{V}_c)$ that shares the same label, then the number of negative eigenvalues of $\mathbf{L}_c \in \mathbb{R}^{(N+K) \times (N+K)}$ is between 0 and $\frac{K(K-1)}{2} + K(|\mathcal{T}(\mathcal{V}_c)| - 1)$.*

One important observation from Theorem 1 is although edges with negative weights are included, \mathbf{L}_c can still be SPD, i.e., $(\mathbf{\Lambda})_{ii} \geq 0$ for all i . In this case, based on (13), $e^{-\mathbf{\Lambda}}$ will remain as a low-pass filtering function. This suggests that UYGCN inherits the feature smoothing property of the classic GCNs [27, 43]. On the other hand, under the scenario such that $\frac{K(K-1)}{2} + K(|\mathcal{T}(\mathcal{V}_c)| - 1) > N + K$, meaning all eigenvalues of \mathbf{L}_c are negative, then $e^{-\mathbf{\Lambda}}$ will behave like a high-pass filtering function. This indicates that UYGCN can induce both smoothing and sharpening dynamics and is thus able to fit both homophilic and heterophilic graphs. Furthermore, the necessary and sufficient condition for the definiteness of \mathbf{L}_c is closely related to the topology of the so-called electrical network [10] of the input graph and is out of the scope of this paper, so we omit it here.

4.4 Impact on Curvatures and Trade-off Relation

Recent studies have verified that the trade-off between OSM and OSQ issues is closely related to the so-called discretized curvatures defined on the edge of the graph [14, 18]. Since additional edges induced by the CNs enrich the higher order structure of the graph i.e., triangles and 4-cycles, thus the direct consequence of this is that the curvature on the edge becomes larger. For example, consider the Augmented Forman curvature [14] defined as

$$FC_3(i, j) := 4 - d_i - d_j + 3|\#_{\Delta}(i, j)|,$$

where $|\#_{\Delta}(i, j)|$ denote as the number of triangles that contain edge (i, j) . If we add one CN, say node k , into the graph, both node i and j will be rewired to connect to the CN, thus naturally we have one

¹We further assume \mathbf{L}_c has distinct eigenvalues.

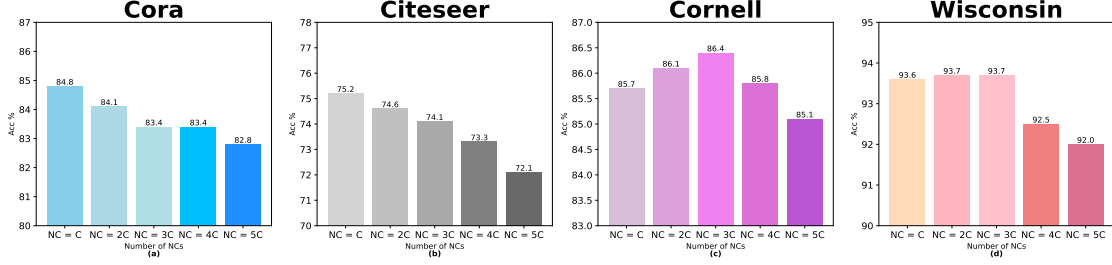


Figure 1: Learning Accuracy of UYGCN with different number of CNs.

additional triangle in the graph. Therefore, the corresponding curvature $FC'_3(i, j)$ on the edge (i, j) becomes $FC'_3(i, j) = 4 - (d_i + 1) - (d_j + 1) + 3(|\#_{\Delta}(i, j)| + 1)$ which is larger than the original $FC_3(i, j)$. Similar conclusions can be drawn when one considers higher-order structures such as 4-cycles. Since negative curvatures are responsible for the OSQ problems [42, 14, 18], and the inclusion of CNs increases curvatures by its induced additional connectivities, therefore naturally mitigates the OSQ problem.

Regarding the OSM issue, intuitively, one can consider the following four situations between original graph nodes i, j , and CNs: (1) The additional CN (denoted as node k for short) has the same label with both nodes i, j ; (2) The label of node k only aligns with one node either from node i or j ; (3) Nodes i and j shares the same label whereas node k is with a different label; (4) All three nodes have different labels. Based on the analogy between GNN propagation and particle systems, one can find that only in situation (1), all three nodes will eventually share the same feature, which is preferred due to their labeling information. In all other situations, nodes with different labels will be pushed away by repulsive forces induced by CNs, which further dilutes the non-desirable attractive forces from their original neighbor that has different labels, suggesting a better fitness compared to the system with no repulsive force, and an analogy of continuous shape deformation of surfaces [25]. However, to appropriately quantify the impact of CNs on the graph curvature as well as the trade-off relation between OSM and OSQ, one shall be required to re-define the curvature over the graph with negatively weighted edges (i.e., sign graphs), we leave this as future work.

5 Experiment

In this section, we conducted numerical experiments to test our proposed models. Specifically, in Section 5.1, we test UYGNNs via three homophilic (Cora, Citeseer, Pubmed) and three heterophilic graphs (Cornell, Texas, Wisconsin) and one large-scale benchmark (Ogbn-Arxiv) [23]. Further in Section 5.2, we analyze the sensitivity of our model to the number of CNs. In addition, in Section 5.3, we show the performance of UYGNNs over long-range graph benchmarks (LRGB) provided in [12] to verify its advantage on the OSQ problem. We provide more experimental details and some additional experiments in Appendix C.

5.1 Node Classification on Homophily/Heterophily Graphs

Setup For the settings in UYGNNs, we initially choose CNs by adding K nodes with their features generated by one layer MLP. For UYGCN, the form of \mathbf{A}_c is used throughout the whole training process, while in UYGAT, the (single-head) attention mechanism is conducted to re-weight \mathbf{A}_c with attention coefficients [43]. For both UYGCN and UYGAT, we normalized \mathbf{A}_c (with self loop) with $\mathbf{D}_c^{-\frac{1}{2}} \mathbf{A}_c \mathbf{D}_c^{-\frac{1}{2}}$, where $(\mathbf{D}_c)_{ii} = \sum_j |(a_c)_{i,j}|$. Both UYGCN and UYGAT are implemented with two layers. The grid search

Table 1: Performance of UYGCN and UYGAT on homophilic, heterophilic, and large scale graph dataset (Arxiv). The best performance is highlighted in **bold** and the second best performance is underlined.

| Methods | Cora | Citeseer | Pubmed | Cornell | Texas | Wisconsin | Arxiv |
|-----------|-----------------|-----------------|-----------------|-----------------|-----------------|-----------------|-----------------|
| MLP | 55.1 | 59.1 | 71.4 | <u>91.3±0.7</u> | 92.3±0.7 | <u>91.8±3.1</u> | 55.0±0.3 |
| GCN | 81.5±0.5 | 70.9±0.5 | 79.0±0.3 | 66.5±13.8 | 75.7±1.0 | 66.7±1.4 | 72.7±0.3 |
| GAT | 83.0±0.7 | 72.0±0.7 | 78.5±0.3 | 76.0±1.0 | 78.8±0.9 | 71.0±4.6 | 72.0±0.5 |
| GIN | 78.6±1.2 | 71.4±1.1 | 76.9±0.6 | 78.0±1.9 | 74.6±0.8 | 72.9±2.5 | 64.5±2.5 |
| APPNP | 83.5±0.7 | <u>75.9±0.6</u> | 79.0±0.3 | 91.8±0.6 | 83.9±0.7 | 92.1±0.8 | 70.3±2.5 |
| H2GCN | 83.4±0.5 | 73.1±0.4 | 79.2±0.3 | 85.1±6.1 | 85.1±5.2 | 87.9±4.2 | 72.8±2.4 |
| GPRGNN | 83.8±0.9 | 75.9±1.2 | 79.8±0.8 | 85.0±5.2 | 75.9±9.2 | 90.4±3.0 | 70.4±1.5 |
| LEGCN | 81.9±2.1 | 73.2±1.4 | 77.4±0.5 | 81.2±3.6 | 81.8±2.9 | 71.5±1.3 | <u>73.3±0.3</u> |
| Replusion | 82.3±0.8 | 71.9±0.5 | 79.3±1.2 | 86.3±2.8 | 83.9±1.5 | 86.6±4.2 | 71.9±0.4 |
| GRAND | 82.9±1.4 | 70.8±1.1 | 79.2±1.5 | 72.2±3.1 | 80.2±1.5 | 86.4±2.7 | 71.2±0.2 |
| SJLR | 81.3±0.5 | 70.6±0.4 | 78.0±0.3 | 71.9±1.9 | 80.1±0.9 | 66.9±2.1 | 72.0±0.4 |
| ACMP | 84.6±0.5 | 75.0±1.0 | 78.0±0.3 | 84.3±4.8 | 85.4±4.2 | 87.8±3.3 | 68.9±0.3 |
| UYGCN | 84.8±0.3 | 75.2±0.4 | 79.9±0.5 | 85.7±1.6 | 88.9±1.5 | 93.6±2.7 | 74.4±0.9 |
| UYGAT | 84.0±0.4 | 76.1±0.8 | <u>79.6±1.5</u> | 87.4±1.3 | <u>89.8±2.5</u> | 89.9±1.8 | 72.3±0.3 |

approach is conducted for fine-tuning model hyperparameters. Both methods are trained with the ADAM optimizer. The maximum number of epochs is 200 for citation networks and heterophilic graphs, whereas 500 for Ogbn-Arxiv. All the datasets follow the standard public split and processing rules. The average test accuracy and its standard deviation come from 10 runs.

Baselines We compare UYGNNs with various baseline models. Except for those classic baseline models such as GCN [27] and GAT [43], we also include some recent works such as LEGCN [49], Repulsive GNN [16], which respectively leverage labeling information and repulsive forces to enhance GNNs performances. Furthermore, we also include SJLR [42], which serves as the initial work of measuring the OSQ problem and resolving it using the graph rewiring paradigm. Finally, we include ACMP, which is the first analogizing the dynamic of GNNs as an evolution of particle systems. All baseline performances are retrieved from public results, and if the results are not available, we implement baseline models to produce the learning accuracy with our best effort.

Results We report the accuracy score percentage with the top 2 highlighted in Table 1. One can find that both UYGCN and UYGAT achieved remarkable learning accuracy compared to the baseline models, especially when compared to their original counterparts, i.e., UYGCN compared to GCN and UYGAT compared to GAT. This observation suggests that our approach of leveraging node labeling information and repulsive force is a model agnostic method to enhance classic GNNs. Furthermore, our models show a good fit on both homophilic and heterophilic datasets thanks to the repulsive forces and the definiteness of graph Laplacian in Theorem 1. Lastly, one can observe that UYGAT is in general with better performances compared to UYGCN in terms of heterophilic graphs, this supports our claim on its *bi-cluster flocking* property that we mentioned in Section 4.1.

5.2 Sensitivity Analysis

In this section, we conduct the sensitivity analysis of UYGCN on the number of CNs. Specifically, we aim to test whether a larger number of negatively weighted edges induced from more CNs will lead to higher

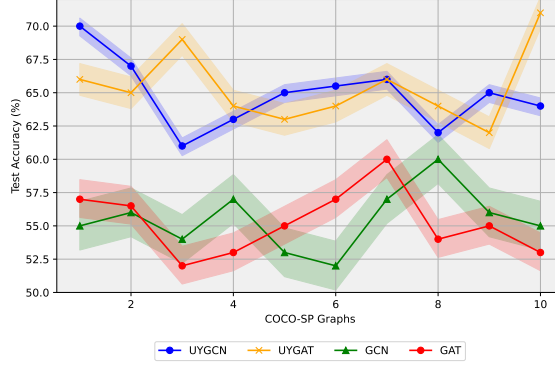


Figure 2: Learning Accuracy (F1 score) of UYGCN, UYGAT and their original models, GCN and GAT on long-term graph benchmarks.

repulsive forces between nodes. In general, adding more CNs to the graph will lead to a higher number of negatively weighted edges unless all labels are evenly distributed. To simplify our analysis, we only test the number of CNs as C , $2C$, $3C$, $4C$, and $5C$. We select Cora, Citeseer, Cornell, and Wisconsin and fix all other model parameters. The learning accuracy is presented in Figure 1. One can observe that for homophilic graphs (Cora and Citeseer), there is a certain amount of accuracy drop with the increase of CNs. This directly verifies that a higher number of CNs introduce more repulsive forces from those newly added negatively weighted edges, making UYGCN less adaptable to homophilic graphs. On the other hand, our model accuracy is even with a slight increase when the number of CNs increases from C to $3C$ via heterophilic graphs. This suggests that more repulsive forces should be preferred for fitting heterophilic graphs. However, with the number of CNs increasing to $4C$ and $5C$, the learning accuracy drops and yields an even worse outcome than $|CNs| = C$. This could be because when $|CNs| = 4C$ and $5C$, the power of double-well potential might not be sufficient to restrict the variations between node features. We highlight that, in this case, one may prefer to deploy a stronger trapping force to the system [45]. Lastly, it is worth noting that a larger number of CNs might be more useful for a graph that contains a large number of nodes, while a small number of distinctive labels, as in this case, one shall prefer to have sufficient “gravitational” sources to induce appropriate attractive and repulsive forces to all nodes.

5.3 Node Classification on Long range Graph Benchmarks.

We test UYGCN and UYGAT over long-range graph benchmarks (LRGBs), namely COCO-SP provided in [12]. The dataset is designed to test whether one GNN model can capture long-range dependency between nodes under the metric of macro F1 score. Specifically, the COCO-SP dataset is a node classification dataset based on the MS COCO image dataset [28] where each superpixel node denotes an image region belonging to a particular class. We highlight that, given the dataset contains over 100000 graphs [12], our purpose for this analysis is to verify that UYGNNs can capture the long-term dependency between nodes in one graph. Therefore, we randomly sample 10 graphs from both datasets and report the average F1 scores. We compare UYGCN and UYGAT to the performance of GCN and GAT, and all models are 4 layers deep. The results are shown in Figure 2. One can find that both UYGCN and UYGAT show superior performance compared to their original counterparts, GCN and GAT, among all selected graphs. This suggests that our proposed approach can dramatically increase the model’s power of capturing long-term dependency between nodes.

6 Related Works

Label Enhanced Approaches in GNNs Node labeling information has been leveraged in recent studies of GNNs to enhance their performance. For example, [44] and [38] utilized labeling information to enrich the node features, followed by the work [9] in which labeling information is leveraged for enhancing GNNs on the long-distance node relations (i.e., OSQ problem). [46] further improved GNNs’ performance using the labels from the outputs of the model. In addition, [47] deployed a topological optimization scheme to propagate labels under fixed points conditions [36], assuming that the nearby vertices in a graph tend to share the same label. Finally, the label-enhanced graph neural network (LEGNN) developed in [49] expands the graph adjacency matrix with node labels and empirically shows the accuracy gain of the GNNs enhanced by their methods.

Dirichlet Energy and OSM The so-called Dirichlet energy and its variants are the commonly applied measurement on the OSM issue of GNNs. Although the OSM issue has been observed for years [6], its commonly accepted definition has just been established recently [31]. Nevertheless, many attempts have been made to mitigate the OSM issue via the lens of dynamic systems [21, 11, 41], multi-scale spectral filtering [22, 33, 48] as well as feature optimizations [34, 15, 50].

Graph Topology and OSQ Unlike the OSM, the OSQ problem has just been identified and quantified recently [2, 42], and little is known about a commonly acceptable definition of the OSQ issue. Despite this, many topological indicators have been spotted to be responsible for the OSQ, for example, graph Ricci/Forman curvature [42, 18], leading to the so-called spatial rewiring approaches. Other indicators such as spectral gap [26], Cheeger constant [3], and effective resistance serve as the motivation of so-called spectral rewiring for the OSQ issue.

7 Concluding Remarks

In this work, we developed a model agnostic approach to enhance GNNs to handle several major challenges via their propagation by leveraging the analogy of particle systems and node labeling information. We verified the properties of our model along with theoretical analysis and various empirical studies. We also investigated the functionality of negative eigenvalues in the graph spectrum from the perspective of heterophilic adaption and the additional edges induced from CNs through the lens of curvature. As CNs bring the training of GNNs in the realm of signed graphs, further exploration of the properties of signed graphs, such as the signed graph “spectral gap” and curvature for measuring the goodness of connectivity are needed [4] to develop more advanced GNN enhancement approaches. We leave these as future works.

References

- [1] Shin Mi Ahn and Seung-Yeal Ha. Stochastic flocking dynamics of the Cucker-Smale model with multiplicative white noises. *Journal of Mathematical Physics*, 51(10), 2010.
- [2] Uri Alon and Eran Yahav. On the bottleneck of graph neural networks and its practical implications. In *International Conference on Learning Representations*, 2020.
- [3] Pradeep Kr Banerjee, Kedar Karhadkar, Yu Guang Wang, Uri Alon, and Guido Montúfar. Oversquashing in GNNs through the lens of information contraction and graph expansion. In *The 58th Annual Allerton Conference on Communication, Control, and Computing*, pages 1–8. IEEE, 2022.
- [4] Francesco Belardo, Sebastian M Cioabă, Jack H Koolen, and Jianfeng Wang. Open problems in the spectral theory of signed graphs. *arXiv:1907.04349*, 2019.
- [5] Mitchell Black, Zhengchao Wan, Amir Nayyeri, and Yusu Wang. Understanding oversquashing in GNNs through the lens of effective resistance. In *International Conference on Machine Learning*, pages 2528–2547. PMLR, 2023.
- [6] Chen Cai and Yusu Wang. A note on over-smoothing for graph neural networks. *arXiv:2006.13318*, 2020.
- [7] José A Carrillo, Massimo Fornasier, Jesús Rosado, and Giuseppe Toscani. Asymptotic flocking dynamics for the kinetic Cucker-Smale model. *SIAM Journal on Mathematical Analysis*, 42(1):218–236, 2010.
- [8] Ben Chamberlain, James Rowbottom, Maria I Gorinova, Michael Bronstein, Stefan Webb, and Emanuele Rossi. Grand: Graph neural diffusion. In *International Conference on Machine Learning*, pages 1407–1418. PMLR, 2021.
- [9] Deli Chen, Xiaoqian Liu, Yankai Lin, Peng Li, Jie Zhou, Qi Su, and Xu Sun. Highwaygraph: Modelling long-distance node relations for improving general graph neural network. *arXiv:1911.03904*, 2019.
- [10] Wei Chen, Ji Liu, Yongxin Chen, Sei Zhen Khong, Dan Wang, Tamer Başar, Li Qiu, and Karl H Johansson. Characterizing the positive semidefiniteness of signed Laplacians via effective resistances. In *The 55th IEEE Conference on Decision and Control*, pages 985–990. IEEE, 2016.
- [11] Francesco Di Giovanni, James Rowbottom, Benjamin P Chamberlain, Thomas Markovich, and Michael M Bronstein. Graph neural networks as gradient flows. *arXiv:2206.10991*, 2022.
- [12] Vijay Prakash Dwivedi, Ladislav Rampásek, Michael Galkin, Ali Parviz, Guy Wolf, Anh Tuan Luu, and Dominique Beaini. Long range graph benchmark. *Advances in Neural Information Processing Systems*, 35:22326–22340, 2022.
- [13] Di Fang, Seung-Yeal Ha, and Shi Jin. Emergent behaviors of the Cucker-Smale ensemble under attractive-repulsive couplings and Rayleigh frictions. *Mathematical Models and Methods in Applied Sciences*, 29(07):1349–1385, 2019.
- [14] Lukas Fesser and Melanie Weber. Mitigating over-smoothing and over-squashing using augmentations of Forman-Ricci curvature. *arXiv:2309.09384*, 2023.

- [15] Guoji Fu, Peilin Zhao, and Yatao Bian. p -Laplacian based graph neural networks. In *International Conference on Machine Learning*, volume 162 of *PMLR*, pages 6878–6917, 2022.
- [16] Jian Gao and Jianshe Wu. Repulsion-GNNs: Use repulsion to supplement aggregation. *IEEE Transactions on Knowledge and Data Engineering*, 35(8):8448–8460, 2022.
- [17] Justin Gilmer, Samuel S Schoenholz, Patrick F Riley, Oriol Vinyals, and George E Dahl. Neural message passing for quantum chemistry. In *International Conference on Machine Learning*, pages 1263–1272. PMLR, 2017.
- [18] Jhony H Giraldo, Fragkiskos D Malliaros, and Thierry Bouwmans. Understanding the relationship between over-smoothing and over-squashing in graph neural networks. *arXiv:2212.02374*, 2022.
- [19] Jhony H Giraldo, Konstantinos Skianis, Thierry Bouwmans, and Fragkiskos D Malliaros. On the trade-off between over-smoothing and over-squashing in deep graph neural networks. *arXiv:2212.02374*, 2022.
- [20] Marco Gori, Gabriele Monfardini, and Franco Scarselli. A new model for learning in graph domains. In *IEEE International Joint Conference on Neural Networks, 2005.*, volume 2, pages 729–734. IEEE, 2005.
- [21] Andi Han, Dai Shi, Lequan Lin, and Junbin Gao. From continuous dynamics to graph neural networks: Neural diffusion and beyond. *arXiv:2310.10121*, 2023.
- [22] Andi Han, Dai Shi, Zhiqi Shao, and Junbin Gao. Generalized energy and gradient flow via graph framelets. *arXiv:2210.04124*, 2022.
- [23] Weihua Hu, Matthias Fey, Marinka Zitnik, Yuxiao Dong, Hongyu Ren, Bowen Liu, Michele Catasta, and Jure Leskovec. Open graph benchmark: Datasets for machine learning on graphs. *Advances in Neural Information Processing Systems*, 33:22118–22133, 2020.
- [24] V Jelic and F Marsiglio. The double-well potential in quantum mechanics: a simple, numerically exact formulation. *European Journal of Physics*, 33(6):1651, 2012.
- [25] Miao Jin, Junho Kim, Feng Luo, and Xianfeng Gu. Discrete surface Ricci flow. *IEEE Transactions on Visualization and Computer Graphics*, 14(5):1030–1043, 2008.
- [26] Kedar Karhadkar, Pradeep Kr. Banerjee, and Guido Montufar. FoSR: First-order spectral rewiring for addressing oversquashing in GNNs. In *International Conference on Learning Representations*, 2023.
- [27] Thomas N Kipf and Max Welling. Semi-supervised classification with graph convolutional networks. *arXiv:1609.02907*, 2016.
- [28] Tsung-Yi Lin, Michael Maire, Serge Belongie, James Hays, Pietro Perona, Deva Ramanan, Piotr Dollár, and C Lawrence Zitnick. Microsoft COCO: Common objects in context. In *The 13th European Conference on Computer Vision*, pages 740–755. Springer, 2014.
- [29] Xiyang Luo and Andrea L Bertozzi. Convergence of the graph Allen–Cahn scheme. *Journal of Statistical Physics*, 167:934–958, 2017.

- [30] F Marsiglio. The harmonic oscillator in quantum mechanics: A third way. *American Journal of Physics*, 77(3):253–258, 2009.
- [31] T Konstantin Rusch, Michael M Bronstein, and Siddhartha Mishra. A survey on oversmoothing in graph neural networks. *arXiv:2303.10993*, 2023.
- [32] Franco Scarselli, Marco Gori, Ah Chung Tsoi, Markus Hagenbuchner, and Gabriele Monfardini. The graph neural network model. *IEEE Transactions on Neural Networks*, 20(1):61–80, 2008.
- [33] Zhiqi Shao, Dai Shi, Andi Han, Yi Guo, Qibin Zhao, and Junbin Gao. Unifying over-smoothing and over-squashing in graph neural networks: A physics informed approach and beyond. *arXiv:2309.02769*, 2023.
- [34] Zhiqi Shao, Dai Shi, Andi Han, Andrey Vasnev, Yi Guo, and Junbin Gao. Enhancing framelet GCNs with generalized p-Laplacian regularization. *International Journal of Machine Learning and Cybernetics*, pages 1–21, 2023.
- [35] Dai Shi, Yi Guo, Zhiqi Shao, and Junbin Gao. How curvature enhance the adaptation power of framelet GCNs. *arXiv:2307.09768*, 2023.
- [36] Dai Shi, Andi Han, Yi Guo, and Junbin Gao. Fixed point Laplacian mapping: A geometrically correct manifold learning algorithm. In *International Joint Conference on Neural Networks (IJCNN)*, pages 1–9. IEEE, 2023.
- [37] Dai Shi, Andi Han, Lequan Lin, Yi Guo, and Junbin Gao. Exposition on over-squashing problem on GNNs: Current methods, benchmarks and challenges. *arXiv:2311.07073*, 2023.
- [38] Yunsheng Shi, Zhengjie Huang, Shikun Feng, Hui Zhong, Wenjin Wang, and Yu Sun. Masked label prediction: Unified message passing model for semi-supervised classification. *arXiv:2009.03509*, 2020.
- [39] Yue Song, David J Hill, and Tao Liu. On extension of effective resistance with application to graph Laplacian definiteness and power network stability. *IEEE Transactions on Circuits and Systems I: Regular Papers*, 66(11):4415–4428, 2019.
- [40] Alessandro Sperduti. Encoding labeled graphs by labeling RAAM. *Advances in Neural Information Processing Systems*, 6, 1993.
- [41] Matthew Thorpe, Tan Minh Nguyen, Hedi Xia, Thomas Strohmer, Andrea Bertozzi, Stanley Osher, and Bao Wang. GRAND++: Graph neural diffusion with a source term. In *International Conference on Learning Representations*, 2022.
- [42] Jake Topping, Francesco Di Giovanni, Benjamin Paul Chamberlain, Xiaowen Dong, and Michael M Bronstein. Understanding over-squashing and bottlenecks on graphs via curvature. In *International Conference on Learning Representations*, 2021.
- [43] Petar Veličković, Guillem Cucurull, Arantxa Casanova, Adriana Romero, Pietro Liò, and Yoshua Bengio. Graph attention networks. In *International Conference on Learning Representations*, 2018.
- [44] Yangkun Wang, Jiarui Jin, Weinan Zhang, Yong Yu, Zheng Zhang, and David Wipf. Bag of tricks for node classification with graph neural networks. *arXiv:2103.13355*, 2021.

- [45] Yuelin Wang, Kai Yi, Xinliang Liu, Yu Guang Wang, and Shi Jin. ACMP: Allen-Cahn message passing for graph neural networks with particle phase transition. *arXiv:2206.05437*, 2022.
- [46] Han Yang, Xiao Yan, Xinyan Dai, Yongqiang Chen, and James Cheng. Self-enhanced GNN: Improving graph neural networks using model outputs. In *International Joint Conference on Neural Networks*, pages 1–8. IEEE, 2021.
- [47] Liang Yang, Zesheng Kang, Xiaochun Cao, Di Jin, Bo Yang, and Yuanfang Guo. Topology optimization based graph convolutional network. In *International Joint Conferences on Artificial Intelligence*, pages 4054–4061, 2019.
- [48] Mengxi Yang, Xuebin Zheng, Jie Yin, and Junbin Gao. Quasi-framelets: Another improvement to graph neural networks. *arXiv:2201.04728*, 2022.
- [49] Le Yu, Leilei Sun, Bowen Du, Tongyu Zhu, and Weifeng Lv. Label-enhanced graph neural network for semi-supervised node classification. *IEEE Transactions on Knowledge and Data Engineering*, 2022.
- [50] Jiayu Zhai, Lequan Lin, Dai Shi, and Junbin Gao. Bregman graph neural network. *arXiv:2309.06645*, 2023.

A Formal Proofs

Proof of Proposition 1. The proof is by contradiction. Suppose that the fixed point of its discrete iteration of (6) is $(\mathbf{c}, \bar{\mathbf{f}})$ with $\mathbf{c} = c\mathbf{I}_N$, then we have

$$\begin{cases} \mathbf{c} = \hat{\mathbf{A}}\mathbf{c} + \hat{\mathbf{C}}\bar{\mathbf{f}}, \\ \bar{\mathbf{f}} = \hat{\mathbf{C}}^\top \mathbf{c} + \mathbf{D}_f^{-1}\bar{\mathbf{f}}, \end{cases}$$

where $\hat{\mathbf{A}} = (\hat{\mathbf{A}}_c)_{1:N, 1:N}$ and $\hat{\mathbf{C}} = (\hat{\mathbf{A}}_c)_{N:N+K, 1:N}$ and $\mathbf{D}_f \in \mathbb{R}^{K \times K}$ be the diagonal degree matrix of the added nodes.

For each added node k , suppose we can find one sample $i \in \mathcal{V}_{\text{tr}}$ such that $y_i = y_k$. Then by the first equation, we have

$$\begin{aligned} Kc &= \bar{f}_1 - \sum_{k \neq 1} \bar{f}_k, \\ Kc &= \bar{f}_2 - \sum_{k \neq 2} \bar{f}_k, \\ &\dots \\ Kc &= \bar{f}_K - \sum_{k \neq K} \bar{f}_k. \end{aligned}$$

This suggests $\bar{f}_1 = \bar{f}_2 = \dots \bar{f}_K = \bar{f} = -\frac{K}{K-2}c$. From the second equation, without loss of generality, we consider a single added node with degree $d = 1 + n^+ + n^-$ where n^+, n^- denote the number of training nodes with a same or different label as the considered node. Hence, this suggests

$$\bar{f} = \frac{1}{d}(n^+ - n^-)c + \frac{1}{d}\bar{f},$$

which leads to $\bar{f} = \frac{n^+ - n^-}{n^+ + n^-} c = -\frac{K}{K-2} c$. This gives rise to a contradiction that $n^+ = -\frac{2}{2K-1} n^- < 0$, because $K \geq 1$. The proof is complete. \square

Proof of Proposition 2. By using the similar way in proving Proposition 1 of [45], we can prove that $\|\mathbf{h}\|_2^2$ is bounded by a constant C depending on the graph size and the largest eigenvalue of the Laplacian \mathcal{L} . Therefore $\mathcal{E}_{\text{dir}}(\mathbf{h}) \leq \lambda_{\max} \|\mathbf{h}\|_2^2 \leq 2C$. \square

Proof of Proposition 3. The proof follows directly from the process used in [5]. If there is no CN either from the nodes of the original graph or additionally added, the above equation is reduced to the conclusion provided in [5]. To show the inclusion of CNs can actually increase the OSQ upper bound, if CNs are selected from the original graph, i.e., the block \mathbf{C} in \mathbf{A}_c disappears, and $|\mathbf{A}_c|$ becomes denser compared to \mathbf{A} due to newly added edges, Therefore it naturally mitigates the OSQ problem according to (12). More specifically, one can verify that if these CNs (selected from the original graph) are not connected to any other nodes, then the maximum number of edges added is $K|\mathcal{T}(\mathcal{V}) - 1|$ where we let $|\mathcal{T}(\mathcal{V})|$ be the number of nodes in the training set in which all nodes labeling information are available. In the worst case, if all of these types of CNs are connected and connected to all other nodes in the training set, then based on (12), same upper bound can be ensured. Similar reasoning can be conducted when CNs are additionally added to the graph, and the number of edges added is fixed as $K|\mathcal{T}(\mathcal{V})| + \frac{K(K-1)}{2}$. Lastly, it is worth noting that in our proof and practical implementations, we only considered two cases that is (1) All CNs are sourced from the graph, and (2) All CNs are new to the graph. For the cases where the source of CNs is mixed, we omit it here for simplicity. \square

Proof of Theorem 1. 1 Denote \mathcal{E}^- all the negative edges in the augmented graph \mathcal{G}_c . Assume that every additional CN has at least one node sharing identical label, then the number of newly added negatively weighted edges connecting the CN would be less than $|\mathcal{T}(\mathcal{V}_c) - 1|$. Since CNs are themselves connected with negative edges, we have $K(K-1)/2$ number of such edges. Therefore the total number of negatively weighted edges $|\mathcal{E}^-| \leq K(K-1)/2 + K|\mathcal{T}(\mathcal{V}_c) - 1|$. Theorem 7 in [39] shows that \mathbf{L}_c has at most $|\mathcal{E}^-|$ negative eigenvalues, which is less than $K(K-1)/2 + K|\mathcal{T}(\mathcal{V}_c) - 1|$ negative eigenvalues. This completes the proof. \square

B Illustration on Cluster Flocking

The notion of cluster flocking is extensively studied in the field of particle systems and mathematical physics [13, 1, 7], serving as a tool for describing the evolution of a system. The famous Cucker-Smale system (CS) is one of the most popular systems that is considered a second-order system adopting classic dynamics. The recent work [13] analyzed the potential bi-cluster flocking behaviors via the CS system with two ensembles with both repulsive and attractive forces that extend the conclusions from the previous studies where only attractive forces were considered. In the context of dynamic systems on graphs, the bi-cluster flocking can be defined in the following way,

Definition 3 (Bi-cluster flocking [45]). For a graph \mathcal{G} , its nodes are said to have a bi-cluster flocking behavior if there exist two disjoint sets of nodes subsets $\mathcal{V}_1 = \{v_i^{(1)}\}_{i=1}^{N_1}$ and $\mathcal{V}_2 = \{v_i^{(2)}\}_{i=1}^{N_2}$ ($N = N_1 + N_2$) on

which the dynamics $\{\mathbf{h}_i^{(1)}(t)\}_{i=1}^{N_1}$ and $\{\mathbf{h}_i^{(2)}(t)\}_{i=1}^{N_2}$ satisfy the following conditions

$$\begin{aligned} \sup_{0 \leq t \leq \infty} \max_{1 \leq i, j \in N_1} |h_i^{(1)}(t) - h_j^{(1)}(t)| &< \infty, \\ \sup_{0 \leq t \leq \infty} \max_{1 \leq i, j \in N_2} |h_i^{(2)}(t) - h_j^{(2)}(t)| &< \infty, \end{aligned} \quad (14)$$

and

$$\exists C', t^* > 0, \text{ s.t. } \forall t > t^*, \max_{1 \leq i \in N_1, 1 \leq j \in N_2} \{|h_i^{(1)}(t) - h_j^{(2)}(t)|\} \geq C', . \quad (15)$$

where $h_i^{(1)}(t)$ and $h_j^{(2)}(t)$ are any single component of vectors $\mathbf{h}_i^{(1)}(t)$ and $\mathbf{h}_j^{(2)}(t)$, respectively.

In the case of its discrete dynamic, the first condition in the above definition suggests given any iteration of the GNN defined on \mathcal{G} , the within-group node feature difference is bounded, whereas the second condition suggests there exists a specific number of layer ℓ^* , after which the between-graph variation will always be greater than a constant C' .

Similar to ACMP, here we briefly illustrate that UYGAT can also achieve bi-cluster flocking. We highlight that given most of the proofs are in general similar to ACMP [45] and the analysis in [13], we will mainly focus on the illustration of our conclusion. However, it is possible to observe bi-cluster flocking via UYGAT in which both attractive and repulsive forces are further reweighed from the attention coefficient, serving as a special type of ACMP in which $\beta_{i,j}$ is learnable rather than a positive constant. Thus according to Proposition 2 in [45], UYGAT has one bi-cluster flocking.

Lastly, it is worth emphasizing again that although both our incoming results and ACMP model illustrate that our models can have node bi-cluster flocking, the necessary and sufficient conditions on how to achieve it are still unknown and worth future exploration.

Let us turn to the UYGCN model with double-well potential with the dynamic as follows,

$$\frac{\partial}{\partial t} \mathbf{h}_i(t) = \sum_{j \in \mathcal{N}_i} a_c(\mathbf{h}_i, \mathbf{h}_j)(\mathbf{h}_j - \mathbf{h}_i) + \delta \mathbf{h}_i(1 - \mathbf{h}_i^2), \quad (16)$$

where for the convenience reason, we denote \mathcal{N}_i as the neighbours of node i in \mathcal{G}_c which is the graph expanded by the CNs. We highlight that in ACMP, a strength coupling (α, δ) is defined to further quantify the attractive and repulsive forces in the system. One can check that UYGCN is a special case of ACMP in terms of the strength coupling where $\alpha = 1$. Next, we quantify bi-cluster flocking according to [45] and [13, 7]. Further, due to the form of \mathbf{A}_c , the edge weights in (16) are ± 1 in front of their components difference. One can see that, based on the setting of UYGCN, the minimum attractive force (+1) is equal to the maximum repulsive force (−1). Therefore, the system is unlikely (but possible) to have bi-cluster flocking.

C Experiment Details

In this section, we provide details of our empirical analysis.

C.1 Performance on Citation and Heterophilic Benchmarks

We start with additional details on the performance of UYGNN and UYGAT via citation networks and heterophilic graphs. The statistics, including their homophily index of the included datasets, are listed in Table 2.

Table 2: Statistics of the datasets, $\mathcal{H}(\mathcal{G})$ represent the level of homophily.

| Datasets | Class | Feature | Node | Edge | $\mathcal{H}(\mathcal{G})$ |
|-----------|-------|---------|--------|---------|----------------------------|
| Cora | 7 | 1433 | 2708 | 5278 | 0.825 |
| Citeseer | 6 | 3703 | 3327 | 4552 | 0.717 |
| PubMed | 3 | 500 | 19717 | 44324 | 0.792 |
| Arxiv | 23 | 128 | 169343 | 1166243 | 0.681 |
| Wisconsin | 5 | 251 | 499 | 1703 | 0.150 |
| Texas | 5 | 1703 | 183 | 279 | 0.097 |
| Cornell | 5 | 1703 | 183 | 277 | 0.386 |

We tuned hyper-parameters using the grid search method for the parameter searching space. The search space for learning rate was in $\{0.1, 0.05, 0.01, 0.005\}$, number of hidden units in $\{16, 32, 64\}$, weight decay in $\{0.05, 0.01, 0.005\}$, dropout in $\{0.3, 0.5, 0.7\}$, the coefficients δ for the double-well potential is initially set as 0 for homophilic graphs and searched in the range of $\{0.5, 1, 1.5, 2, 2.5\}$ for heterophilic graphs.

Furthermore, we observed that doing normalization on \mathbf{A}_c can improve UYGCN’s performance in general. This could due to the fact that the normalization scheme $\mathbf{D}_c^{-\frac{1}{2}} \mathbf{A}_c \mathbf{D}_c^{-\frac{1}{2}}$ brings the degree information of the nodes to reweight \mathbf{A}_c , causing the imbalance between repulsive and attractive forces according to the definition of cluster flocking, and such imbalance may lead the system to cluster flocking. This provides the insights explaining the benefit of doing normalization on graph adjacency matrix even with negative weights.

An additional interesting discovery in our empirical study is in some heterophilic graphs, i.e., *Cornell*, where we have a limited number of nodes. It is possible to have nodes in its training set obtained from the random split which don’t cover all type of labels, i.e., total number of distinct labels in the training set less than C . In this case, the power of CNs will be largely diluted since there will be some CNs that do not induce any additional connections. In this case, we report the learning results of the average learning accuracy (10 times) on the training set that contains all types of labels.

C.2 LRGB Experiment

We provide more descriptions on COCO-SP datasets and the implementation details on conducting our test on it. The COCO-SP dataset is a node classification dataset based on the MS COCO image dataset [28] where each superpixel node denotes an image region belonging to a particular class. Based on [12], there are 123,286 graphs with a total of 58.7 million nodes in COCO-SP where each corresponds to an image in MS COCO dataset. The graphs prepared after the superpixels extraction have on average 476.88 nodes, with mean degree 5.65 and totally 332,091,912 edges with average edges of 2693.67 per graph. The evaluation metric for COCO-SP is the macro F1 score.

Same as the reason mentioned in our main paper, since the main purpose for us to conduct UYGNNs on LRGB is to verify its advantage of capturing long-term relationships between nodes, we only randomly select 10 graphs from COCO-SP and report the learning accuracy of our models and their original counterparts. Different from the LRGB experiment conducted in some graph rewiring papers, for each selected, we maintained the split ratio as 20% for training, 20% for validation, and the rest for testing, thus resulting in a higher F1 score compared to [12, 14]. Furthermore, to conduct a fair comparison, we set all hyper-parameters the same in the LRGB experiment.